Journal Name

ARTICLE TYPE

Cite this: DOI: 10.1039/xxxxxxxxxx

Hysteresis Phenomena in Perovskite Solar Cells: the Many and Varied Effects of Ionic Accumulation

Daniel A. Jacobs*[a], Yiliang Wu[a], Heping Shen[a], Chog Barugkin[a], Fiona J. Beck[a], Thomas P. White[a], Klaus Weber[a] and Kylie R. Catchpole[a]

Received Date
Accepted Date

DOI: 10.1039/xxxxxxxxxx

www.rsc.org/journalname

The issue of hysteresis in perovskite solar cells has now been convincingly linked to the presence of mobile ions within the perovskite layer. Here we test the limits of the ionic theory by attempting to account for a number of exotic characterization results using a detailed numerical device model that incorporates ionic charge accumulation at the perovskite interfaces. Our experimental observations include a temporary enhancement in open-circuit voltage following prolonged periods of negative bias, dramatically S-shaped current-voltage sweeps, decreased current extraction following positive biasing or "inverted hysteresis", and non-monotonic transient behaviours in the dark and the light. Each one of these phenomena can be reproduced and ultimately explained by our models, providing further evidence for the ionic theory of hysteresis as well as valuable physical insight into the factors that coincide to bring these phenomena about. In particular we find that both interfacial recombination and carrier injection from the selective contacts are heavily affected by ionic accumulation, and are essential to explaining the non-monotonic voltage transients and S-shaped J-V curves. Inverted hysteresis is attributed to the occurrence of "positive" ionic accumulation, which may also be responsible for enhancing the stabilized open-circuit voltage in some perovksite cells.

Introduction

Initially a speculation put forward to explain the notorious issue of current-voltage hysteresis,[1] the hypothesis that mobile ions are a significant player in perovskite solar cells (PVSCs) is now supported by several direct lines of evidence.[2–5] Akin to a dynamic doping profile, the presence of these ions has the potential to profoundly affect device performance, and complicates the interpretation of even the simplest cell characterization tools. Current-voltage (J-V) characterization has become particularly contentious due to its direct bearing on cell efficiency,[6] but many other measurements exhibit unusual transient behaviour as well.[4,7–9] The persistence of these phenomena in standard TiO_2/$MAPbI_3$/Spiro-OMeTAD cells necessitates a thorough understanding of the myriad ways in which mobile ions could affect standard electro-optical measurements. Such an understanding may be relevant to both the ultimate performance of perovskite cells as well as to their interim behaviour in the lab.

Numerical device modelling at the level of the basic semiconductor equations is an effective first approach to understanding the consequences of ionic motion under minimal assumptions. To date modelling efforts have been primarily concerned with explaining the sweep-rate and pre-conditioning dependence of standard J-V measurements,[10,11] emphasizing the importance of a compensated internal electric field.[12] In this picture the primary effect of ion migration is to screen or compensate the electric field within the perovskite layer by accumulating at its interfaces, dramatically affecting carrier distributions and hence the photovoltaic current. Since the internal field is determined by applied bias as well as the cell's built-in potential, mobile ions will be accumulated at the interfaces to different degrees de-

[a] *Centre for Sustainable Energy Systems, Research School of Engineering, The Australian National University, Canberra, Australian Capital Territory, Australia.*
* *E-mail: daniel.jacobs@anu.edu.au*

† Electronic Supplementary Information (ESI) available: [details of any supplementary information available should be included here]. See DOI: 10.1039/b000000x/

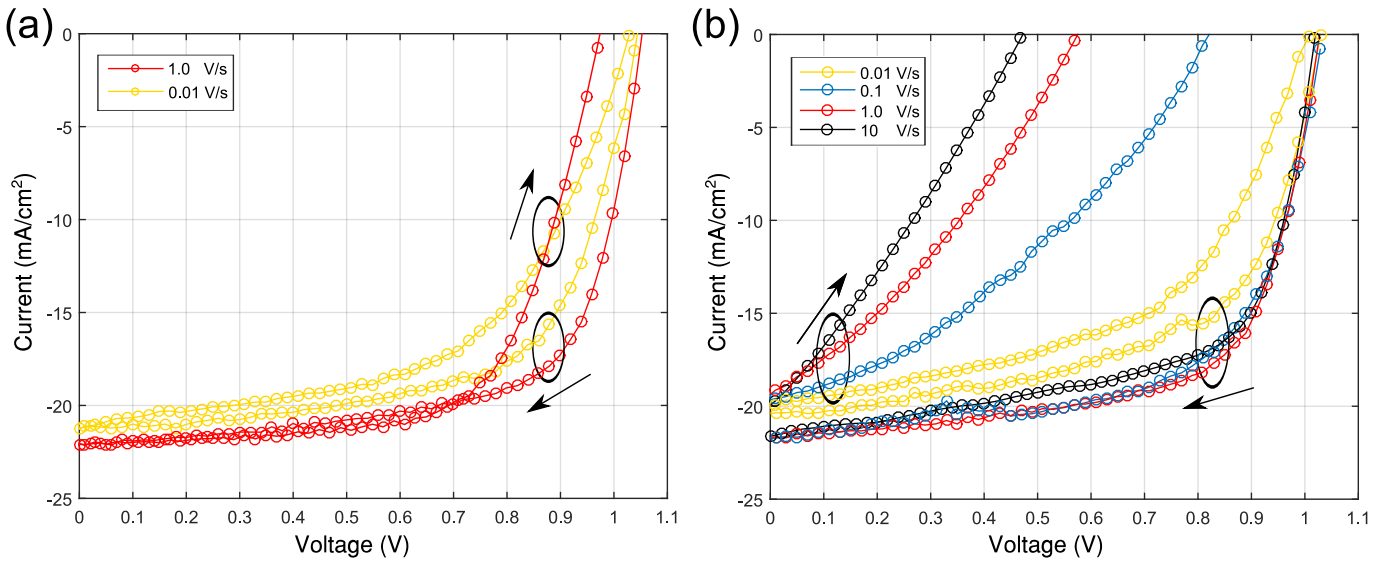

Fig. 1 (a) J-V sweeps showing clear signs of hysteresis, taken following periods of open-circuit biasing before each scan. Here the optimal scan rate is ambiguous, complicating comparisons between cells. (b) Rapid scan current-voltage measurements taken after pre-biasing at short-circuit (forward scan) and the stabilized open-circuit voltage (reverse scan). The trends with increasing scan rate are clearer, and appear to approach a limit representing cell performance under static accumulation.

pending on the cell's biasing history. As a starting point, the concept of a compensated electric field caused by ion accumulation accounts for the fundamental experimental observation of transiently lower current extraction following biasing periods at negative potential [13,14] (i.e. $V < V_{\mathrm{built-in}} \approx 1\,\mathrm{V}$). Yet there remain a number of phenomena for which a basic understanding in terms of the compensated electric field proves insufficient, and it is necessary to consider in detail the effect of ion migration on carrier injection, accumulation and recombination. Here we provide experimental evidence that a number of such phenomena occur in TiO_2/$MAPbI_3$/Spiro-OMeTAD solar cells. We provide mechanistic explanations for these phenomena based on numerical device modelling, showing that the ionic theory can account for a variety of unusual electrical measurements beyond the standard rate-dependant J-V sweeps.

Methods

Rapid-scan characterization

In order to simplify comparisons between experiment and simulation, we begin by describing a non-standard measuring protocol. [12] J-V hysteresis in PVSCs is typically characterized by measuring forward and reverse scans after pre-biasing periods near open-circuit [13,14] (authors differ in their choice of whether to perform the forward scan immediately after the reverse scan or following an additional biasing period, but this is of little concern here). The splitting between the forward and reverse J-V curves is used to gauge the severity of hysteresis, sometimes quantitatively with the use of an index. [15,16] Whilst informative, such measurements suffer from the drawback that the scanning rate determines the degree to which a cell is able to equilibrate at each bias voltage, and can give misleading results if chosen either too high or too low. The response is effectively frozen in a scan which is too fast , whereas in a slow scan the cell comes close to reaching equilibrium at each bias voltage, with both cases leading to reduced or even negligible splitting of the forward and reverse J-V curves. At some intermediate scanning rate the difference between forward and reverse scans should reach a maximum, but the task of finding this maximal scan rate may require a large number of measurements. In any case the dependence on scan rate complicates the process of assessing the degree of hysteresis in a given cell.

An alternative procedure that mostly avoids the scan-rate dependence involves allowing the cell to equilibrate at two distinct "pre-bias" voltages (0 V and the stabilized open-circuit voltage make natural choices), instead of a single one, before performing rapid J-V scans over the range of interest. The hope is that the ions will be effectively frozen in their initial positions if these J-V scans are performed rapidly enough, so that the resulting data represents the cell's performance under two distinct static distributions of ions instead of a time-varying distribution which evolves over the course of the measurement. A comparison of the more common "forward-reverse sweep" with rapid-scan measurements made on our mesoporous TiO_2/$MAPbI_3$/Spiro-OMeTAD cells shows that the latter method is indeed far more effective at manifesting the hysteretic behaviour (Fig. 1(a,b)). The large splitting between forward and reverse scans taken at a rapid

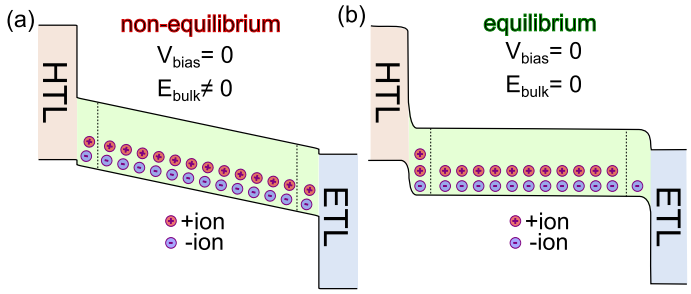

Fig. 2 Schematic band diagram of the perovskite solar cell depicting how the motion of a single mobile species (positive here) leads to the accumulation of net positive and negative doping concentrations at the two interfaces, whilst the perovskite remains an intrinsic semiconductor in its bulk. In (a) the ions are shown in non-equilibrium positions with respect to the internal field whereas in (b) the internal field is screened after accumulation in layers of fixed width, and equilibrium is reached.

speed demonstrates that these cells are profoundly affected by the pre-biasing conditions, and manifests qualitative features which beg for explanation (for instance, dramatically diminished voltages on the forward scan which we address shortly). The rapid-scan measurements also simplify the process of interpretation and comparison with simulation, as it is only necessary to compute two ionic distributions rather than performing fully transient simulations. The cells used in these experiments were relatively slow to stabilize, with typical settling times in the range of 10-100 s, and as a result scan rates of around $10\,\mathrm{V\,s^{-1}}$ were found to be sufficient for the rapid-scan characterization.

SCAPS Model

To fully understand the behaviour seen in these rapid-scan results we developed an ionic device model using SCAPS.[17] In this model the perovskite solar cell (apart from its mobile ions) is envisaged as an n-i-p heterojunction device governed by the usual drift-diffusion equations of semiconductor physics. This entails some simplification, particularly since the cells fabricated for our experiments all incorporate mesoporous a TiO_2 scaffold on the n-type contact. Nevertheless, we obtain good qualitative agreement by using only a single planar n-type contact layer in the models. Recombination is taken to be predominately trap-mediated (SRH type) with contributions from both bulk defects as well as surface states at the Spiro-OMeTAD/$MAPbI_3$ (HTL/ABS) and $MAPbI_3$/TiO_2 (ABS/ETL) interfaces. The interfacial defects allow for holes in the HTL to recombine directly with electrons in the perovskite (along with the analogous process at the ABS/ETL interface), which proves to be an important feature referred to hereafter as "surface recombination". The main model parameters are given in the ESI.†

Ions are input as doping concentrations localized within narrow layers located adjacent to the two perovskite interfaces, with concentration determined by an equilibrium condition at the pre-bias voltage. The perovskite layer is assumed to be intrinsic on average, meaning that the mobile ions are compensated by an equal number of homogenously distributed stationary defects of opposite charge, as in Schottky disorder. The net doping which arises in the accumulation regions therefore corresponds to an accumulation of ions on one side and a depletion of ions on the other (Fig. 2). For simplicity the widths of the accumulation and depletion zones (hereafter "accumulation zones"), which are likely to differ in reality,[11] are set equal, making the model agnostic about the charge of the mobile species. These simplifications are discussed further in the supplementary information (Fig. S1†).

The condition we use for equilibrium at a given bias voltage is that the bulk electric field within the perovskite (outside the accumulation zones) should be fully screened when the ions reach their resting positions, which assumes that the density of mobile ions is high enough for full screening to occur. Applied to the motion of ions a drift-diffusion balance implies that higher ionic densities will form narrower accumulation zones at equilibrium.[11] Our calculations suggest that densities above approximately $10^{17}\,\mathrm{cm^{-3}}$ result in full screening and accumulation in zones less than 50nm wide (Fig. S1a†). We note that mobile vacancy concentrations above $10^{19}\,\mathrm{cm^{-3}}$ have been predicted for $MAPbI_3$.[18] At smaller concentrations ($< 10^{17}\,\mathrm{cm^{-3}}$) these regions spread outwards into the bulk and the concept of an accumulation zone loses its meaning. Once determined by the equilibrium condition, the distribution of ions is held fixed over a full J-V scan. This is meant to simulate measuring the cell over a time interval shorter than that of ionic relaxation. Because SCAPS calculates equilibrium properties at each bias voltage, the contribution of capacitive currents[19] is neglected in the J-V results presented herein. We have performed calculations comparing the total charge stored within cells under different conditions of accumulation which suggest that these capacitive corrections to the current are negligible within our assumptions.

Experimental

Cells were fabricated according to the standard FTO/compact-TiO_2/mesoporous-TiO_2/$MAPbI_3$/spiro-OMeTAD/Au structure.¶ The measurements presented here represent a collection of what we believe are interesting results spanning several batches, and in each case were chosen to best exhibit the effect in question. Apart from batch-to-batch variation, the only major difference between cells concerns the preparation of the compact titania layer: cells in Figs. 1,4,6,7 incorporated a solution-processed layer whereas those in Figs. 5, 6 were made via atomic layer deposition (ALD). The full implications of this difference in

¶ Full experimental details are given in the ESI†.

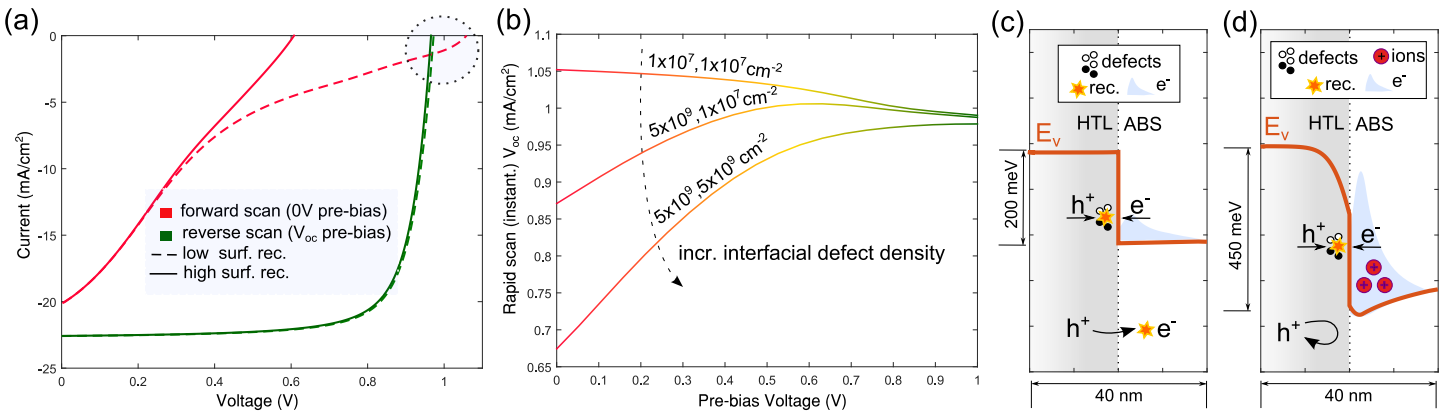

Fig. 3 (a) Simulated rapid-scan characteristics (at instantaneous speed) for cells with high (solid) and low (dotted) rates of surface recombination corresponding to different pre-biasing voltages (equivalently degrees of negative ionic accumulation). The effect of surface recombination is most obvious in the forward scan open-circuit voltage which may be either enhanced or diminished compared to the reverse scan depending on the interfacial defect density. (b) Simulated trends in instantaneous open-circuit voltage versus pre-bias voltage showing qualitatively different behaviour depending on the interface defect density (labels correspond to defect densities at the HTL/ABS and ABS/ETL interfaces respectively). (c,d) Simulated valence band energies at open-circuit conditions near the HTL/Perovskite interface with (d) and without (c) accumulated ions, indicating that negative ionic accumulation suppresses injection from the HTL into the ABS layer, in addition to enhancing surface recombination (denoted 'rec.' in the figure) at large forward bias due to carrier build-up. Analogous processes are expected at the ABS/ETL interface.

preparation are beyond the scope of this paper and form the subject of an ongoing investigation. Although we focus on cells made with pure $MAPbI_3$, the approach and mechanisms considered here are general and should apply equally to cells with mixed and inorganic compositions, provided they retain the essential feature of possessing slow mobile ions at a sufficient density to influence cell behaviour.

Results and Discussion

Surface recombination and carrier injection

To begin our analysis we address the suggestion that hysteresis in PVSCs cannot be attributed to mobile ions alone, but is due to a specific combination of mobile ions and interfacial traps or recombination centres.[10] In that study it was argued that whilst purely bulk recombination is capable of accounting for standard hysteresis behaviour, the required rate constants are unphysically high. We also find that surface recombination is an apparently necessary feature, but for different reasons which play an essential role in the results to follow.

Examples of simulated rapid-scan J-V measurements are shown in Fig. 3a subject to different degrees of surface recombination. From these results it is clear that surface recombination has a strong influence on the forward scan at high forward bias, and particularly affects its intercept or open-circuit voltage (V_{oc}). Without surface recombination the predicted forward scan voltage often exceeds that of the reverse scan, as shown in Fig. 3a (dotted lines), which contradicts the experimental trend represented in Fig. 1a. With added surface recombination (solid lines) the correct trends result, particularly in terms of the voltage, which is then drastically diminished in rapid scans following negative pre-biasing, as in experiment. The discrepancy between experiment and our simulated result with only bulk recombination in Fig. 3a suggests that the effect of surface recombination is apparently vital. In the following we will rationalize this observation by arguing that there are two competing effects of ion accumulation which influence the instantaneous open-circuit voltage: enhanced recombination due to the compensated field, and suppressed carrier injection into the perovskite from the contact layers. Under certain circumstances this competition can in fact lead to higher open-circuit voltages under ionic accumulation, a somewhat surprising prediction which we confirm in our transient V_{oc} measurements discussed later (Fig. 7).

In order to present the argument that accumulated ions can enhance cell voltage it is helpful to introduce some terminology: here and in the following "negative ionic accumulation" is used to denote the state in which ions are distributed with positive ions located on the HTL side and negative ions on the ETL side of the absorber layer. Negative accumulation is to be expected if a cell is left to equilibrate at negative "internal bias" $(V - V_{\mathrm{built-in}}) < 0$.‡ Since a good cell should have $V_{\mathrm{built-in}} \approx 1\,\mathrm{V}$, most bias voltages in the power-generating quadrant of the J-V plane will cause negative ionic accumulation at equilibrium. Negative accumulation usually has a negative impact on cell performance, manifesting as instantaneously lower current extraction for cells pre-biased at 0V as compared to those pre-biased at V_{oc} (e.g. Fig. 1a). This

‡ as V refers to the potential difference across the perovskite layer the contribution of series resistances occurring elsewhere in the cell is not included.

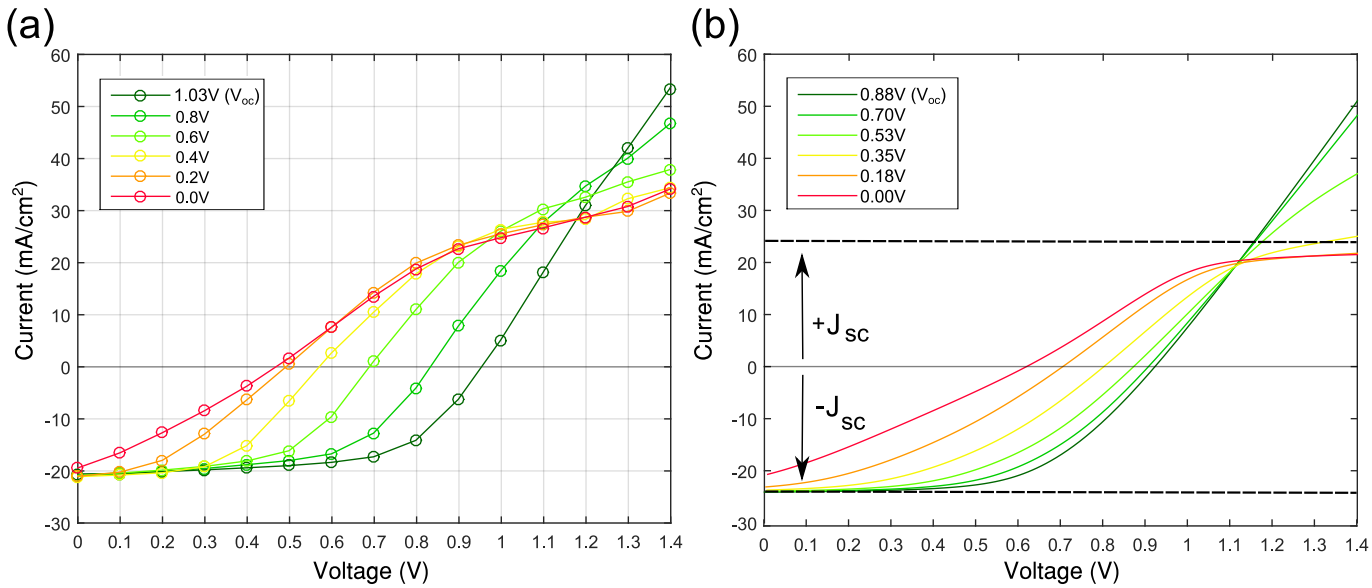

Fig. 4 (a) Rapid (20V/s) forward scan measurements taken after equilibration at different pre-bias voltages, showing S-shaped saturation features at high forward bias. (b) Simulated J-V curves under different conditions of ionic accumulation corresponding to pre-bias voltages shown in the legend. In this model a series resistance of 8Ω cm^2 was added to approximate the slope of the experimental curves at large bias.

comes about because ions in negative accumulation screen the built-in field that would normally sweep photo-generated carriers out of the cell. However, the accumulation of ions also affects the heterojunction interfaces between the perovskite and selective blocking layers. Under negative accumulation the positive ions at the HTL side can be thought of as constituting a depleted n-doped region, analogous to a pn-junction, leading to a strong depletion of contact carriers near each interface as illustrated for the HTL/ABS interface in Fig. 3d. Therefore negative accumulation is expected to reduce current injection into the perovskite layer as compared to cells without accumulation (Fig. 3c), a prediction which is confirmed later via measurements of the dark current in our cells (Fig. 6).

Since V_{oc} can be identified as the bias point at which the collected current is balanced by a competing forward current, suppressed injection should lead to a higher cell voltage (assuming equal collection). In cells modelled with bulk defects but a negligible density of surface defects this indeed occurs, as current injection from the contacts is the only mechanism by which a forward current can flow. However, and to the contrary, cells with a high density of surface defects can also sustain a forward current through the direct recombination between photo-generated carriers in the absorber and carriers in the selective contacts ("surface recombination"). This surface recombination is enhanced by negative ionic accumulation as a consequence of carrier build-up and tends to reduce the open-circuit voltage (Fig. 3d illustrates the electron build-up which occurs under negative accumulation at the HTL/ABS interface). In fact it is probable that this voltage loss under negative accumulation occurs mostly within the narrow accumulation layers, causing a decoupling of the bulk quasi-fermi level splitting from the terminal voltage (which has important implications for photoluminescence imaging[20]). Surface recombination is therefore important in the modelling because it allows a forward current to flow despite the injection barriers which appear under negative accumulation, giving the correct prediction of reduced voltages under severe negative accumulation. We note that a high forward current could also flow under negative accumulation if there are shunt pathways within a device, but these cannot be used account for the S-shaped J-V scans considered shortly.

Different instances of the competition between injection and recombination under negative accumulation are demonstrated in Fig. 3b which shows the rapid-scan or instantaneous V_{oc} versus pre-bias voltage for cells with varying interfacial defect densities. These calculations show explicitly that without a significant density of interfacial defects there is a increasing trend in instantaneous open-circuit voltage with decreasing pre-bias voltage (equivalent to increasing negative ionic accumulation), whereas with high defect densities the trend is reversed. Interestingly, at intermediate densities a non-monotonic trend emerges which can be invoked to explain our measurement of non-monotonic transient open-circuit voltage (Fig. 7) discussed below.

S-shaped J-V scans at high forward bias

We now turn to a separate but closely related rapid-scan measurement that reinforces two central ideas in the discussion above: namely that negatively accumulated ions suppress carrier injection from the contacts, and that the presence of surface states at both interfaces can allow photogenerated carriers to flow in the "wrong" (forward) direction in PVSCs. By extending the range of our rapid-scan protocol beyond V_{oc} we obtained evidence that both of these effects occur simultaneously in some cells. The rapid-scan measurements of Fig. 4a manifest S-shaped* current-voltage characteristics for cells pre-biased at voltages less than 0.8 V. The location of the saturation features at approximately $J = +J_{sc}$ (using the sign convention that $J(0\,\mathrm{V}) = -J_{sc}$) strongly suggests that the cell's photocurrent is flowing in the forward instead of the reverse direction at high forward bias. This alone indicates significant surface recombination at both interfaces, without which it would be impossible for photocurrent to flow in the forward direction due to the large interface band offsets. The fact that the current increases only very slowly above $J = +J_{sc}$ after pre-biasing at low voltages further indicates that there must be high barriers to injection which inhibit the forward current from growing further. We were able to simulate this phenomenon (Fig. 4b) in cells given a significant density of surface states at both interfaces (recombination velocity $\geqslant 10\,\mathrm{cm\,s^{-1}}$). This is apparently vital to reproducing the effect: only cells with both accumulated ions and surface recombination at both interfaces exhibit a forward current which saturates at $J = +J_{sc}$. Cells with high interfacial defect densities but without accumulated ions retain their built-in field, which prevents the flow of photocurrent in the forward direction. On the other hand cells with high ion accumulation but a low density of interfacial defects can only drive a forward current via the injection pathway, and therefore there is also no S-shaped feature (Fig. S2a†). The measurement of Fig. 4a can therefore be regarded as simultaneous evidence for ionic accumulation and significant surface recombination at both perovskite interfaces.

Effect of positive accumulation

So far we have only considered negative ionic accumulation, which should occur when a PVSC with mobile ions is left to equilibrate at bias voltages less than the cell's built-in potential ($V < V_{built-in}$). Negative accumulation tends to reduce fill factors, J_{sc} and V_{oc}, and is therefore harmful to cell efficiency, although simulations indicate that it may lead to marginally higher open-circuit voltages under certain conditions as discussed above. The opposite state of positive accumulation may also come about if the cell is allowed to rest at positive pre-bias voltages satisfying $V > V_{built-in}$. Positive accumulation is generally expected to improve cell performance according to the observation that reverse scans usually exhibit instantaneously higher currents, voltages and fill factors in PVSCs (e.g. Fig. 1b). In Fig. 5a we show a set of measurements that partially violate this expectation by exhibiting lower J_{sc} in the rapid scans following forward pre-biasing, despite having higher open-circuit voltages. For this cell the effect is quite pronounced; another measurement showing a more subtle version of the same effect on a different cell is given in the ESI (Fig. S3†). The simulations accompanying this measurement are given in Fig. 5b, which shows similar fast-sweep current-voltage curves under different degrees of both positive and negative ionic accumulation. We note that in this simulation a drastic reduction in J_{sc} under positive accumulation only emerges under high ion densities corresponding to equilibrium at approximately 1.5 V rather than the lower value of $V_{oc} \approx 1\,\mathrm{V}$ as in the measurement, although there are signs of the same effect at lower densities (1.3 V pre-bias in the figure).§ The discrepancy in pre-bias voltages between measurement and simulation could have a number of causes, but points to a deficiency in the equilibrium condition used for determining the ionic accumulation (which could be altered by the presence of additional contributions to the internal field such as that of trapped or accumulated carriers at the interface). Any other effect which would act to enhance the detrimental effect of positive accumulation could also be responsible.

Lowered current extraction following positive biasing has been reported recently under the name of "inverted hysteresis",[21] in which the authors invoke a reversed band-ordering at one of the interfaces to explain the phenomenon. The simulations presented here use the usual band ordering as in Fig. 2a and therefore preclude this explanation at least for our simulated result; instead the phenomenon can be understood directly by observing the simulated band diagrams under different conditions of accumulation as shown in Figs. 5(c,d). These simulated band diagrams show that extraction barriers at the perovskite interfaces can develop under high degrees of positive accumulation (left of Fig. 5(c) circled). These regions of reversed electric field or unfavourable band bending trap carriers near the wrong interface, causing increased surface recombination and hence reduced J_{sc}. The degree of the band bending is strongly affected by parameters such as the perovskite's dielectric constant and the band offsets, providing at

* The sense in which these are 'S-shaped' differs somewhat from previous usage: here the curves extend to high forward bias and the "levelling off" occurs at positive rather than zero current.[12]

§ This accounts for why the effect does not appear the in the simulation of Fig. 4b which extends to a maximum pre-bias voltage of only 0.88 V. We cannot at present say why the measurements of Fig. 4a failed to show the same effect, but this may be related to a preparation difference in the compact titania layer (solution-processed versus ALD, see the ESI†).

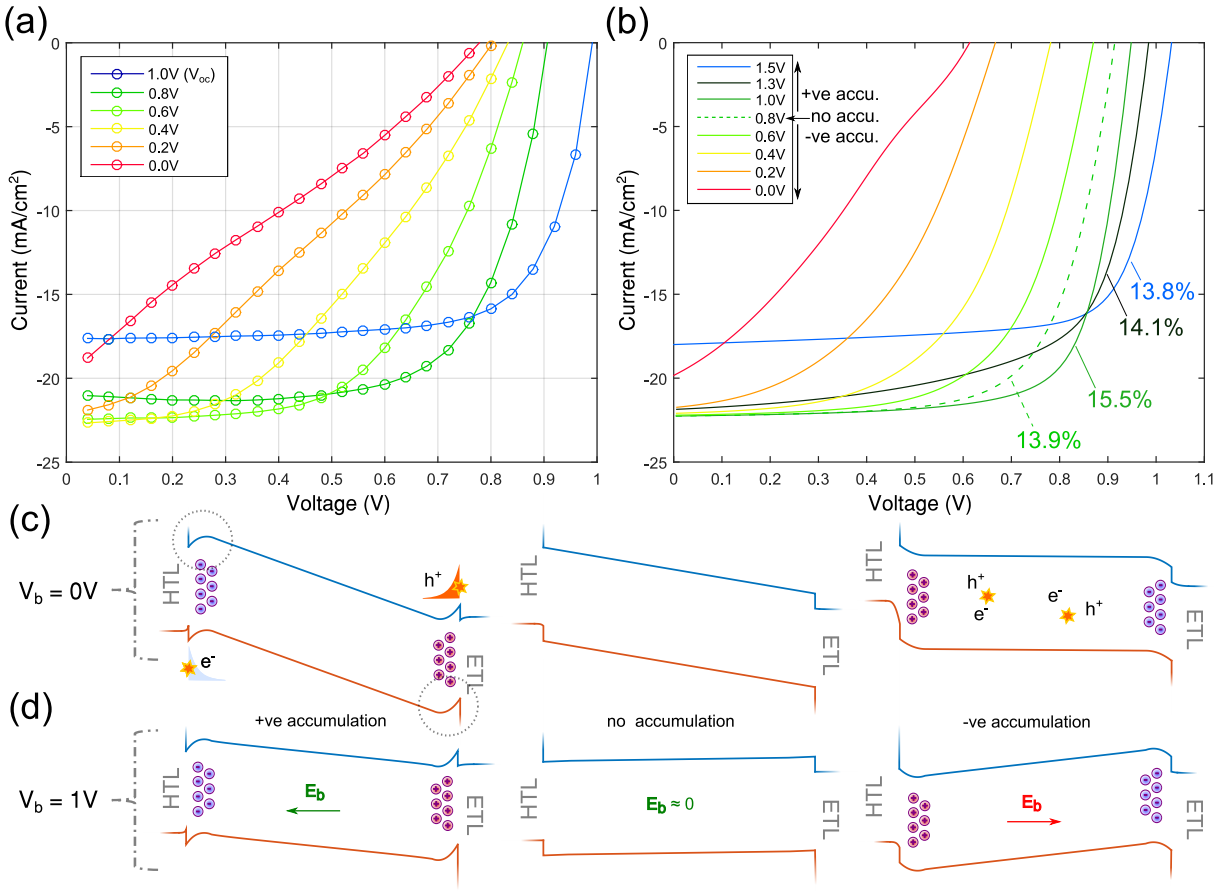

Fig. 5 (a) Rapid forward scan measurements (20V/s) taken after equilibration at different bias voltages given in the legend. These results exhibit reduced J_{sc} after forward biasing, or "inverse hysteresis". (b) Simulated forward scans showing the joint effects of positive and negative ion accumulation: negative accumulation reduces V_{oc} and J_{sc}, whilst positive accumulation enhances V_{oc}, but at the cost of J_{sc} under extreme positive accumulation (1.5V pre-bias in our model). Power conversion efficiencies for some of the curves are shown in the labels. (c,d) Simulated band diagrams at 0V (c) and 1V (d) bias demonstrating the effects of positive (left) and negative (right) ionic accumulation, as compared with no accumulation (middle). Surface recombination caused by unfavourable band-bending (circled) reduces J_{sc} under severe positive accumulation, whilst the screened electric field under negative accumulation causes a similar reduction due to increased bulk recombination. At high forward bias the cell under positive accumulation enjoys the benefit of an enhanced bulk electric field (E_b) which enlarges the voltage as compared cells under no or negative accumulation.

least two examples of parameters which could influence the outcome of positive accumulation. Naturally we find that the effect is much reduced in models with a lower density of surface states (see Fig. S2b†). The same accumulation responsible for the loss in current causes an enhancement of the bulk electric field however, which contributes to a simultaneous improvement in cell voltage (Fig. 5(d)). Indeed, our simulations for a small excess of positive accumulation tend to show higher conversion efficiencies than cells with either negative or no accumulation (Fig. 5b, labels) due to improvements in V_{oc} and fill factor. Despite their slightly higher power conversion efficiencies, the cells under positive accumulation shown in Fig. 5b would not be at ionic equilibrium at their maximum power points. Depending on the cell parameters our models can predict both positive and negative accumulation at the stabilized maximum power point, leading respectively to slightly enhanced and reduced conversion efficiencies, and an ambiguous answer as to how ions affect the stabilized efficiency of PVSCs.

If it is correct to attribute the reduction in J_{sc} seen in the fast scan measurements of Fig. 5a to positive ionic accumulation, then it is noteworthy that the cell measured in Fig. 5a shows reduced J_{sc} after pre-biasing at only 0.8 V. This suggests that positive accumulation is already occurring at 0.8 V, and therefore that $V_{built-in} < 0.8$ V (by comparison the simulated cell of Fig. 5b has a built-in voltage of 0.82 V). If true this would imply that significant positive accumulation is occuring at the stabilized $V_{oc} \approx 1$ V, which could therefore be considerably enhanced over its "bare value" by the presence of accumulated ions, as suggested by the trend that higher cell voltages occur in cells under positive accumulation (Fig. 5b). This leads us to speculate that positive ionic accumulation could be a contributor to the high open-circuit voltages of some PVSCs. Although the difference between the open-circuit voltage without ions (914 mV) and in equilibrium with ions (933 mV, not shown) is hardly appreciable in the model of Fig. 5b, it must be noted that this model apparently underestimates the effects of positive accumulation quite significantly (given the discrepancy in pre-bias voltages noted earlier), implying the potential for larger enhancements in real cells.

Simulations with dynamic accumulation

Further insight into the consequences of ionic accumluation can be gained by measuring cells at a fixed bias, over time, following pre-biasing periods under different conditions. Here we report on two such measurements: one is a measurement of the dark current evolution in a cell pre-biased into negative accumulation, and another is a measurement of the photo-voltage transient following the onset of illumination. The former confirms our prediction that negative accumulation can suppress carrier injection into the cell, whilst the latter provides an explicit demonstration of the voltage enhancement under mild negative accumulation discussed earlier. These simulations were carried out by using MATLAB to perform successive SCAPS simulations using a time-varying ionic charge according to $dN_{ion}/dt \propto E_{bulk}$ where E_{bulk} represents a typical electric field in the perovskite layer. The timescale was left arbitrary to reflect our uncertainty about the ionic mobility, as well as other possible influences on the slow charging such as the role of the contact layers.[22]

Fig. 6a shows the dark current evolution for two different cells measured at a fixed forward bias (1 V) after equilibration at 0 V in the dark. Under these conditions the ions are expected to begin in a state of negative accumulation before relaxing towards either a state of positive accumulation or approximate neutrality. In both cells the dark current is observed to increase dramatically over the course of this relaxation, supporting the idea that negatively accumulated ions inhibit carrier injection into the perovskite layer, and consistent with previous results.[23] However, an unexpected feature emerged which is that cells prepared with different compact TiO_2 layers repeatedly exhibited different qualitative trends: while cells prepared with atomic layer deposition (ALD) compact (cp-) TiO_2 layers were found to respond faster and with a non-monotonic transient (Fig. 6a, dotted line), cells with a spin-coated cp-TiO_2 layer responded more slowly and monotonically (Fig. 6a, solid line). The difference in cp-TiO_2 layer preparation was determined to affect the compact layer's n-type doping level, which motivated a search for cell parameters that could account for both behaviours under a simple change in ETL doping. Such models were found, and the results from one of these are shown in Fig. 6b. We find that the non-monotonic behaviour can be attributed to trap-filling in cells with predominantly SRH-type non-radiative recombination. This is supported by the observation that cells simulated with purely radiative recombination always show monotonic trends under ionic accumulation (Fig. S5†). In the model of Fig. 6b we include only one SRH recombination source for clarity, which is chosen to lie at the HTL/ABS interface. In this case the non-monotonic current evolution for the cell with low ETL doping can be traced to a switch-over in the limiting carrier for surface recombination from holes in the HTL to electrons in the absorber. A detailed explanation is given below.

In their initial state of negative accumulation, the ions cause a build-up of electrons at the HTL/ABS interface and a depletion of holes in the HTL layer, making holes the limiting species for recombination (Fig. 6c: t=0). As the ions relax, the depletion decreases and more holes become available for recombination, initially enhancing the dark current in both cells (Fig. 6c: 0<t<15). Meanwhile the surplus of electrons at the HTL interface decreases with time following the restoration of the cell's built-in field. In the cell with low ETL doping this decrease in electron density at the HTL interface eventually becomes the bottleneck for recombination, causing a gradual decrease in the dark current (Fig. 6c: t>15). The cell with higher ETL doping injects relatively more

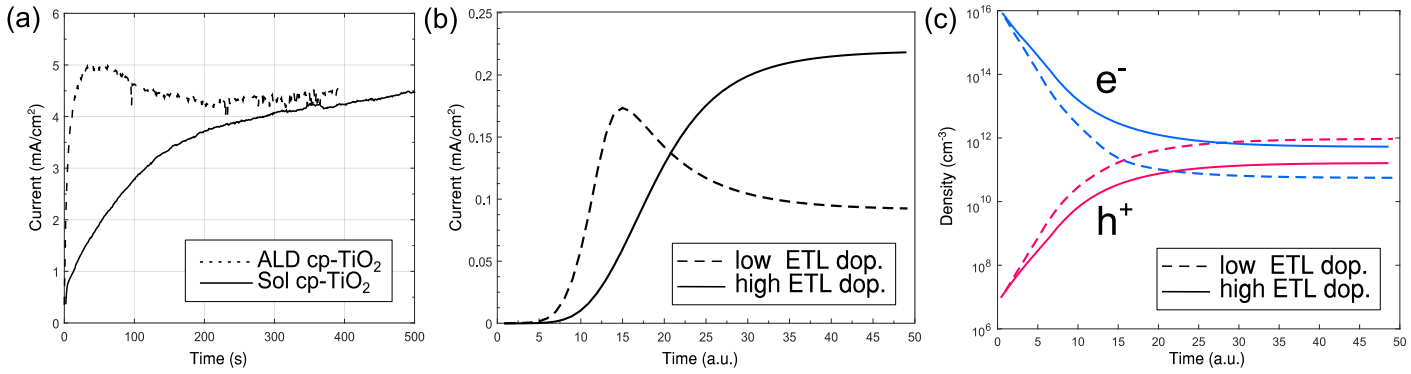

Fig. 6 (a) Transient measurement of the dark current for cells pre-biased at $0\,\mathrm{V}$, measured at $1\,\mathrm{V}$. (b) Simulated dark current transients for the same biasing procedure (measured at $0.6\,\mathrm{V}$ due to numerical instability) predicting the non-monotonic trend in cells with low ETL doping. (c) Simulated electron and hole densities at the HTL/Perovskite interface. The electron densities are measured on the perovskite side and holes on the HTL side, making these the relevant carrier densities for surface recombination as defined earlier.

electrons into the absorber layer however, so that holes remain the bottleneck carrier throughout the evolution and there is no switch-over. The non-monotonic behaviour therefore results once again from a competition between ionic effects on the internal electric field (which influenced the electron concentration at the interface in this example) and the injection of carriers into the absorber. In the supplementary information (Fig. S5) we show that a non-monotonic dependence on ion accumulation also appears in models with bulk rather than surface SRH recombination, but not in those with purely radiative recombination for which there is no concept of a limiting carrier.

Enhancement of transient photovoltage by ionic accumulation

Recording the evolution of a cell's open-circuit voltage after switching from dark to illuminated conditions often results in a monotonic increase in V_{oc} over time, which follows expectations based on the compensated field caused by negative ionic accumulation in the dark: namely, that this accumulation causes initially enhanced recombination and therefore lowered voltage until the ions relax under the influence of the forward bias $V = V_{\mathrm{oc}}$. Somewhat contrary to this expectation, we find that certain cells exhibit an increase in voltage followed by subsequent decay as shown in Fig. 7a. Such non-monotonic voltage transients have also been reported in other recent work[21,24] and represent repeatable, genuine transient behaviour rather than evidence of permanent degradation. It is worth mentioning that these non-monotonic voltage transients have been observed in both pure as well as mixed halide perovskite cells in our lab. We propose that this behaviour can also be explained by mobile ions through the competition between contact-carrier injection and recombination discussed previously. Simulations of the voltage transient were carried out to support this hypothesis, an example of which is given in Fig. 7b. These results exhibit a non-monotonic trend in the open-circuit voltage resembling that seen in the experimental data, despite the ions moving in only one direction from a state of negative accumulation. Indeed, the non-monotonic behaviour mirrors that shown in Fig. 2b for the cell with an intermediate level of surface recombination. The simulated result can be explained by noting that at $t = 0$ the cell begins in a state of high negative accumulation, leading to severe recombination and therefore reduced voltage. After an initial relaxation stage the surface recombination is reduced, and the remaining ions act to suppress carrier injection, causing a temporary enhancement in voltage lasting until they fully relax to equilibrium.

In terms of dynamics there are obvious discrepancies between theory and experiment in Figs. 6 and 7, with fast initial rises showing in the measurements but not in our simulations. This is suggestive of additional complexity in the accumulation process which is absent in the models, such as the presence of multiple ionic species, or a coupling between ionic accumulation and some other slow charging process which is triggered by changes in bias and/or illumination.[22]

Conclusions

We have developed numerical device models to demonstrate that the ionic theory is viable as an inclusive account for hysteresis phenomena in PVSCs, and not just the basic observations about rate-dependent J-V sweeps. Rapid-scan J-V characterization was used as a tool to unveil a number of unexpected behaviours relating to J-V hysteresis. This scanning protocol may not have a direct bearing on stabilized cell efficiency, but provides a window into the physical processes going on within the cell and can provide useful clues to fuel more specific investigations. The observation of S-shaped rapid scans provides strong evidence that significant interfacial recombination can occur at both the TiO_2/$MAPbI_3$ and $MAPbI_3$/Spiro-OMeTAD interfaces. The occurrence of "in-

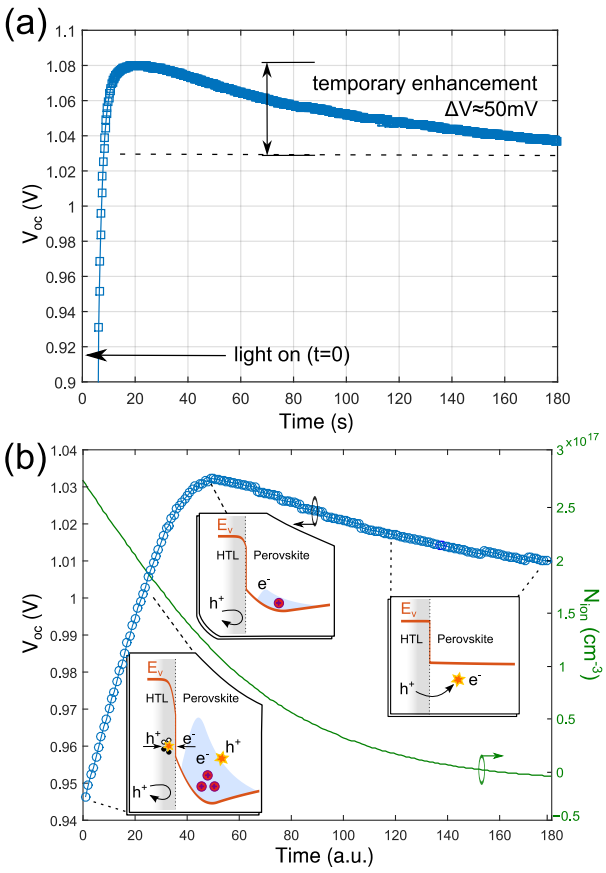

Fig. 7 (a) Measurement of V_{oc} evolution after switching on illumination at t=0 (part of the fast initial rise for $t < 5\,s$ is omitted). We interpret the maximum value as a temporary enhancement over the stabilized voltage caused by negative ionic accumulation. (b) Simulated V_{oc} (blue circles) showing non-monotonic behaviour despite the monotonically decreasing ionic charge (green line). For this cell $V_{built-in} \approx 1V$, causing the ionic charge to settle to approximate neutrality ($V_{built-in} - V_{oc} \approx 0$). Insets illustrate the competition between recombination and carrier injection responsible for the temporary enhancement.

verted hysteresis" was explained in terms of the ionic accumulation caused by biasing cells above their built-in potential. We propose that such "positive accumulation" may be responsible for enhancing the stabilized open-circuit voltage of some perovskite solar cells, although the effect of ions on stabilized efficiency remains unclear. A numerical model using SCAPS predicts a negligible contribution to the hysteresis behaviour from capacitive currents, but is nonetheless able to account for our rapid-scan measurements surprisingly well. This suggests that capacitive contributions may be unimportant to the slow hysteresis behaviour in PVSCs. The importance of surface recombination in explaining voltage trends, S-shaped curves and the inverted hysteresis effect further justifies a previously suggested link between interfacial trap states and hysteresis, and represents one reason to expect suppressed signatures of hysteresis in high performing cells.

Finally, non-monotonic transient behaviour in open-circuit voltage and dark current was also reproduced in a transient version of our numerical model, providing compelling evidence that these phenomena are also caused by ionic accumulation. The rate of these processes is however not well predicted by the ionic theory alone, pointing to contributions from additional charging processes occurring at the interfaces, or perhaps to the existence of multiple mobile species. Nonetheless, given the number of explanatory successes this theory now enjoys, it seems likely that any microscopically distinct hypothesis for the origin of hysteresis in perovskite cells (such as that of ferroelectric behaviour) will have to resemble its device-level implications very closely. The unintuitive nature of many of the results presented here suggests that the possible contributions of mobile ions to exotic behaviour in PVSCs should be carefully considered before invoking new physical phenomena.

References

1 A. Dualeh, T. Moehl, N. Tétreault, J. Teuscher, P. Gao, M. K. Nazeeruddin and M. Grätzel, *ACS Nano*, 2014, **8**, 362–73.

2 C. Li, S. Tscheuschner, F. Paulus, P. E. Hopkinson, J. Kießling, A. Köhler, Y. Vaynzof and S. Huettner, *Advanced Materials*, 2016, **28**, 2446–2454.

3 Y. Yuan, J. Chae, Y. Shao, Q. Wang, Z. Xiao, A. Centrone and J. Huang, *Advanced Energy Materials*, 2015, **5**, 1–7.

4 D. W. DeQuilettes, W. Zhang, V. M. Burlakov, D. J. Graham, T. Leijtens, A. Osherov, V. Bulovic, H. J. Snaith, D. S. Ginger and S. D. Stranks, *Nat Commun*, 2016, **7**, 11683.

5 Y. Shao, Y. Fang, T. Li, Q. Wang, Q. Dong, Y. Deng, Y. Yuan, H. Wei, M. Wang, A. Gruverman, J. Shield and J. Huang, *Energy & Environmental Science*, 2016, **9**, 1752–1759.

6 J. A. Christians, J. S. Manser and P. V. Kamat, *Journal of Physical Chemistry Letters*, 2015, **6**, 852–857.

7 Y. Tian, M. Peter, E. Unger, M. Abdellah, K. Zheng, T. Pullerits, A. Yartsev, V. Sundström and I. G. Scheblykin, *Physical*

chemistry chemical physics : PCCP, 2015, **17**, 24978–24987.

8 X. Fu, D. Jacobs, F. Beck, T. Duong, H. Shen, K. Catchpole and T. White, *Phys. Chem. Chem. Phys.*, 2016, **18**, 22557–22564.

9 R. S. Sanchez, V. Gonzalez-Pedro, J. W. Lee, N. G. Park, Y. S. Kang, I. Mora-Sero and J. Bisquert, *Journal of Physical Chemistry Letters*, 2014, **5**, 2357–2363.

10 S. Van Reenen, M. Kemerink and H. J. Snaith, *Journal of Physical Chemistry Letters*, 2015, **6**, 3808–3814.

11 G. Richardson, S. O'Kane, R. G. Niemann, T. Peltola, J. M. Foster, P. J. Cameron and A. Walker, *Energy Environ. Sci.*, 2016, **9**, 1476–1485.

12 W. Tress, N. Marinova, T. Moehl, S. M. Zakeeruddin, N. Mohammad K., M. Grätzel, M. K. Nazeeruddin and M. Grätzel, *Energy Environ. Sci.*, 2015, **8**, 995–1004.

13 H. J. Snaith, A. Abate, J. M. Ball, G. E. Eperon, T. Leijtens, N. K. Noel, S. D. Stranks, J. T. W. Wang, K. Wojciechowski and W. Zhang, *Journal of Physical Chemistry Letters*, 2014, **5**, 1511–1515.

14 E. L. Unger, E. T. Hoke, C. D. Bailie, W. H. Nguyen, A. R. Bowring, T. Heumüller, M. G. Christoforo and M. D. McGehee, *Energy & Environmental Science*, 2014, **7**, 3690–3698.

15 H. S. Kim and N. G. Park, *Journal of Physical Chemistry Letters*, 2014, **5**, 2927–2934.

16 R. S. Sanchez and E. Mas-Marza, *Solar Energy Materials and Solar Cells*, 2016.

17 M. Burgelman, P. Nollet and S. Degrave, *Thin Solid Films*, 2000, **361**, 527–532.

18 A. Walsh, D. O. Scanlon, S. Chen, X. G. Gong and S. H. Wei, *Angewandte Chemie - International Edition*, 2015, **54**, 1791–1794.

19 O. Almora, C. Aranda, I. Zarazúa, A. Guerrero and G. Garcia-Belmonte, *ACS Energy Letters*, 2016, **1**, 209–215.

20 Y. Wu, H. Shen, D. Walter, D. Jacobs, T. Duong, J. Peng, L. Jiang, Y.-B. Cheng and K. Weber, *Advanced Functional Materials*, 2016.

21 W. Tress, J. P. Correa Baena, M. Saliba, A. Abate and M. Graetzel, *Advanced Energy Materials*, 2016, 1600396.

22 I. Levine, P. K. Nayak, J. Tse, W. Wang, N. Sakai, S. Van Reenen, T. M. Brenner, S. Mukhopadhyay, H. J. Snaith, G. Hodes, D. Cahen and S. V. Reenen, *J. Phys. Chem. C*, 2016, **120**, 16399–16411.

23 B. Wu, K. Fu, N. Yantara, G. Xing, S. Sun, T. C. Sum and N. Mathews, *Advanced Energy Materials*, 2015.

24 P. Calado, A. M. Telford, D. Bryant, X. Li, J. Nelson, C. Brian, O. Regan and P. R. F. Barnes, *arXiv:cond-mat.mat-sci/1606.00818*.